Chiang, T. Olson, J. Dice, *J. Biol. Chem.* **267**, 9202 (1992); H. Wiech, J. Buchner, M. Zimmermann, R. Zimmermann, U. Jakob, *ibid.* **268**, 7414 (1993).

4. T. Chappell, B. Konforti, S. Schmid, J. Rothman, *J. Biol. Chem.* **262**, 746 (1987); K. Milarski and R. Morimoto, *J. Cell Biol.* **109**, 1947 (1989); U. Haus *et al.*, *EMBO J.* **12**, 3763 (1993).
5. K. Flaherty, C. DeLuca-Flaherty, D. McKay, *Nature* **346**, 623 (1990).
6. T. Wang, J. Chang, C. Wang, *J. Biol. Chem.* **268**, 26049 (1993).
7. S. Huang, M. Tsai, Y. Tzou, W. Wu, C. Wang, *ibid.*, p. 2063; M. Tsai and C. Wang, *ibid.* **269**, 5958 (1994).
8. X. Zhu *et al.*, *Science* **272**, 1606 (1996).
9. S. Blond-Elguindi *et al.*, *Cell* **75**, 717 (1993).
10. A. Fourie, J. Sambrooks, M. J. Gething, *J. Biol. Chem.* **269**, 30470 (1994).
11. A. Gragerov, L. Zeng, X. Zhao, W. Burkholder, M. Gottesman, *J. Mol. Biol.* **235**, 848 (1994).
12. Ssa proteins function in protein translocation into organelles and regulation of the heat shock response (*2*). Ssb1 and Ssb2 are 99% identical and are associated with translating ribosomes (*17*); Δ*ssb1* Δ*ssb2* cells are sensitive to cold and to certain translation-inhibiting drugs such as hygromycin B. Reduced numbers of polysomes, previously reported in Δ*ssb1* Δ*ssb2* cells (*17*), are a general characteristic of slowly growing cells (*24*). Ssa and Ssb proteins are each unable to rescue the phenotypes of the other, even when Ssa1 is expressed from the *SSB1* promoter, or vice versa (*2*).
13. Chimeras were generated using Nde I and Xho I sites created by polymerase chain reaction (PCR) at codons 368 and 540 in *SSA1* and 374 and 547 in *SSB1*, respectively. The sites are in regions of Ssa1-Ssb1 identity and did not alter the amino acid sequence or function of either protein. The Nde I site occurs in the final α helix of the 44-kD ATPase domain (*5*). The Xho I site occurs in the long α helix shared by the 18-kD peptide-binding domain and the 10-kD variable domain, at the point of flexibility between them (*8*).
14. Chimeras were named with three-letter acronyms indicating the protein domains they contain. For example, BAB contains the 44-kD ATPase domain of Ssb1, the 18-kD peptide-binding domain of Ssa1, and the 10-kD variable domain of Ssb1.
15. G. Flynn, J. Pohl, M. Flocco, J. Rothman, *Nature* **353**, 726 (1991).
16. P. James, C. Pfund, E. A. Craig, data not shown.
17. R. J. Nelson, T. Ziegelhoffer, C. Nicolet, M. Werner-Washburne, E. Craig, *Cell* **71**, 97 (1992).
18. The chimera ABA could not be tested because it comigrates with Ssa1 protein.
19. The chimera BBA rescued hygromycin B sensitivity but did not detectably associate with polysomes in this assay. It is possible that BBA associates only weakly with polysomes, allowing rescue of the hygromycin B phenotype, but that the complex does not survive the conditions of our analysis.
20. It is unlikely that a single site of function is shared, because both phenotypes were rescued even when ABB was single copy and BAA was overexpressed from a high-copy plasmid.
21. Domain interactions vary for different functions. Growth at low temperature requires primarily the ATPase domain of Ssb, whereas ribosome association depends on interaction at several sites, with each domain contributing to overall binding. These interactions are likely additive, because any one can be lost or weakened by replacement with Ssa sequences without losing Ssb-specific function.
22. D. Cyr, T. Langer, M. Douglas, *Trends Biochem. Sci.* **19**, 176 (1994).
23. The DnaJ homolog Sis1 appears to be a likely partner for Ssb, because it is associated with polysomes. However, Sis1 stimulates the ATPase activity of Ssa1, but not that of Ssb1, in vitro (T. Ziegelhoffer and E. Craig, unpublished data).
24. C. Waldron, R. Jund, F. Lacroute, *Biochem. J.* **168**, 409 (1977).
25. Polysomes were prepared and fractionated as described (*17*) from the Δ*ssb1* Δ*ssb2* strain JN208, except that gene fusions were present on centromeric plasmids and cells were grown in complete synthetic media minus uracil (SC − ura media) to an optical density of 1.0 at 600 nm. Gradient fractions were immunoblotted with a mixture of two antibodies to the COOH-termini of Ssa1 and Ssb1.
26. We thank R. Aramayo, J. Dahlberg, C. Fox, P. Kiley, and M. Krebs for helpful discussions. Supported by grants from NIH (E.A.C. and C.P.) and the Jane Coffin Childs Fund (P.J.).

Chaotic Dynamics in an Insect Population

R. F. Costantino, R. A. Desharnais,* J. M. Cushing, Brian Dennis

A nonlinear demographic model was used to predict the population dynamics of the flour beetle *Tribolium* under laboratory conditions and to establish the experimental protocol that would reveal chaotic behavior. With the adult mortality rate experimentally set high, the dynamics of animal abundance changed from equilibrium to quasiperiodic cycles to chaos as adult-stage recruitment rates were experimentally manipulated. These transitions in dynamics corresponded to those predicted by the mathematical model. Phase-space graphs of the data together with the deterministic model attractors provide convincing evidence of transitions to chaos.

The mathematical theory of nonlinear dynamics has led population biology into a new phase of experimental and theoretical research (*1–6*). Explanations of observed fluctuations of population numbers now include dynamical regimes with a variety of asymptotic behaviors: stable equilibria, in which population numbers remain constant; periodic cycles, in which population numbers oscillate among a finite number of values; quasiperiodic cycles, which are characterized by aperiodic fluctuations that are constrained to a stable attractor called an invariant loop; and chaos, where population numbers change erratically and the pattern of variation is sensitive to small differences in initial conditions. There is, however, a need for new experiments to confirm these hypothetical possibilities (*7*, *8*). A key theoretical prediction, which is subject to experimental challenge, is that specific sequences of transitions among qualitatively different dynamical regimes occur in response to changing biological parameters (*9*, *10*). Here, we address a route to chaos predicted by a mathematical model of insect populations (*11*) in which the onset of chaos is preceded by transitions from stable equilibrium to quasiperiodic and periodic cycles.

We modeled the relation of larval, pupal, and adult *Tribolium* numbers at time $t + 1$ to the numbers at time t by means of a system of three stochastic difference equations:

$$L_{t+1} = bA_t \exp(-c_{el}L_t - c_{ea}A_t + E_{1t}) \quad (1)$$

$$P_{t+1} = L_t(1 - \mu_l)\exp(E_{2t}) \quad (2)$$

$$A_{t+1} = [P_t \exp(-c_{pa}A_t) + A_t(1 - \mu_a)]\exp(E_{3t}) \quad (3)$$

In this model (*12*, *13*), L_t is the number of feeding larvae (referred to as the L-stage) at time t; P_t is the number of large larvae, nonfeeding larvae, pupae, and callow adults (collectively the P-stage) at time t; and A_t is the number of sexually mature adults (A-stage animals) at time t. The unit of time is 2 weeks; this is the approximate average amount of time spent in the L-stage under our experimental conditions, as well as the approximate average duration of the P-stage. The quantity $b > 0$ is the number of larval recruits per adult per unit of time in the absence of cannibalism. The fractions μ_l and μ_a are the larval and adult rates of mortality in one time unit. The exponential nonlinearities account for the cannibalism of eggs by both larvae and adults and the cannibalism of pupae by adults. The fractions $\exp(-c_{el}L_t)$ and $\exp(-c_{ea}A_t)$ are the probabilities that an egg is not eaten in the presence of L_t larvae and A_t adults in one time unit. The fraction $\exp(-c_{pa}A_t)$ is the survival probability of a pupa in the presence of A_t adults in one time unit. The terms E_{1t}, E_{2t}, and E_{3t} are random noise variables assumed to have a joint multivariate normal distribution with a mean vector of zeros and a variance-covariance matrix denoted by Σ. The noise variables represent unpredictable departures of the observa-

R. F. Costantino, Department of Biological Sciences, University of Rhode Island, Kingston, RI 02881, USA.
R. A. Desharnais, Department of Biology and Microbiology, California State University, Los Angeles, CA 90032, USA.
J. M. Cushing, Department of Mathematics, University of Arizona, Tucson, AZ 85721, USA.
B. Dennis, Department of Fish and Wildlife Resources and Division of Statistics, University of Idaho, Moscow, ID 83844, USA.

*To whom correspondence should be addressed. E-mail: bob@biol1next.calstatela.edu

tions from the deterministic skeleton (resulting from environmental and other causes) and are assumed to be correlated with each other within a time unit but uncorrelated through time. These assumptions were found acceptable for many previous data sets (12, 13) by standard diagnostic analyses of time-series residuals (14). The deterministic skeleton of the model is identified by setting $\Sigma = 0$, or, equivalently, by letting E_{1t}, E_{2t}, and E_{3t} equal zero in Eqs. 1 to 3.

We experimentally set the adult mortality rate at $\mu_a = 0.96$ and manipulated recruitment rates into the adult stage, $P_t \exp(-c_{pa}A_t)$, at values that predicted, on the basis of our earlier work (13), a sequence of transitions from a stable equilibrium to quasiperiodic and periodic cycles to chaos: c_{pa} = 0.0, 0.05, 0.10, 0.25, 0.35, 0.50, and 1.0. There was also an unmanipulated control treatment. Twenty-four cultures of the RR strain of *T. castaneum* were initiated with 250 small larvae, five pupae, and 100 young adults. Three populations were randomly assigned to each of the eight treatments. Each population was maintained in a half-pint (237 ml) milk bottle with 20 g of standard media and kept in a dark incubator at 32°C. Every 2 weeks the L-, P-, and A-stages were censused and returned to fresh media, and dead adults were counted and removed. This procedure was continued for 80 weeks. Adult mortality was set by removing or adding adults at the time of a census to make the fraction of adults that died during the interval equal to 0.96. Re-

cruitment rates into the adult stage were manipulated by removing or adding young adults at the time of a census to make the number of new adult recruits consistent with the treatment value of c_{pa}. At the end of every other census, the adults that were returned to the populations were obtained from separate stock cultures maintained under standard laboratory conditions to counter the possibility of genetic changes in life-history characteristics.

We fitted Eqs. 1 to 3 to the time-series data from all 24 cultures by means of maximum likelihood parameter estimation (12). The control and c_{pa}-manipulated cultures were given different variance-covariance matrices in the likelihood function because the experimental manipulations tended to alter the stochastic variability of the populations. The model described the data well.

Using the deterministic skeleton ($\Sigma = 0$) and the parameter estimates (15), we calculated the bifurcation diagram and the (dominant) Liapunov exponents (Fig. 1). A bifurcation diagram is a plot of the asymptotic population numbers versus one of the model parameters; it shows how changes in the parameter affect population dynamics. Solid bands are caused by quasiperiodicity or chaos, and open areas containing lines are the result of periodic cycles. The Liapunov exponent is a measure of the exponential rate of conver-

gence or divergence of nearby initial conditions averaged over the asymptotic attractor. Stable equilibria and periodic cycles will have a negative Liapunov exponent; quasiperiodic invariant loops will have a Liapunov exponent of zero; and a chaotic attractor will have a positive Liapunov exponent. Thus, a positive Liapunov exponent is a signature of chaos. The interval c_{pa} = 0.423 to 0.677 is a region of multiple attractors, with a stable period-3 cycle coexisting with chaos or stable cycles of period 8 or higher. In this region the asymptotic dynamic depends on the initial condition. Contrary to the idea that chaotic dynamics may lead to extinction (16), the bifurcation diagram (Fig. 1) reveals that extinction is unlikely for these populations even in regions of chaotic dynamics.

The parameter estimates (15) placed the experimental treatments in regions of different asymptotic dynamics, as indicated by the arrows in Fig. 1. The c_{pa} = 0.0 treatment is in a region of stable equilibria, as is the unmanipulated control treatment (not shown in Fig. 1). The c_{pa} = 0.05 and c_{pa} = 1.0 treatments are in regions of stable 8- and 3-cycles, respectively. In these two cases, the Liapunov exponents are negative. For the c_{pa} = 0.10 treatment the Liapunov
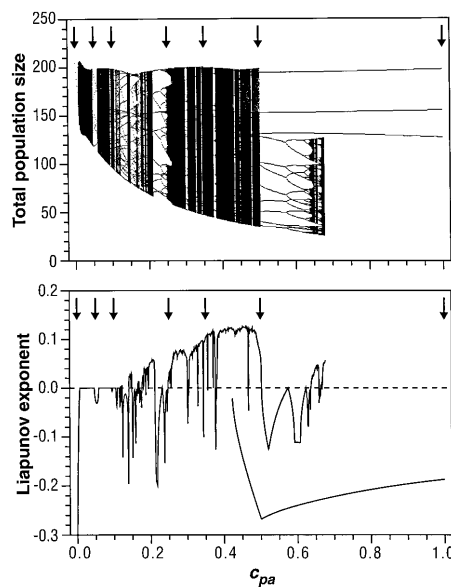

Fig. 1. Bifurcation diagram for total population numbers (L-stage + P-stage + A-stage) and the Liapunov exponents computed using the deterministic skeleton (Eq. 1 with $\Sigma = 0$) and the maximum likelihood parameter estimates (15). The arrows indicate the experimental treatments.
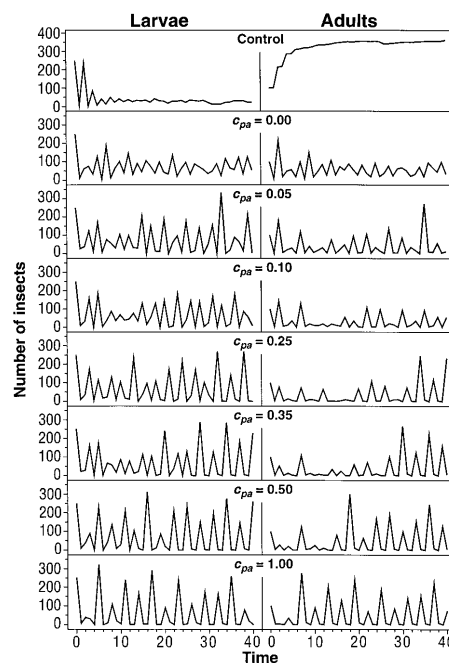

Fig. 2. Time-series data for one replicate from the control and each of the experimental treatments. Numbers of larvae are plotted on the left; numbers of adults are plotted on the right. Numbers of P-stage animals were omitted from these plots because their dynamics closely resemble those of the larvae. One time unit equals 2 weeks.
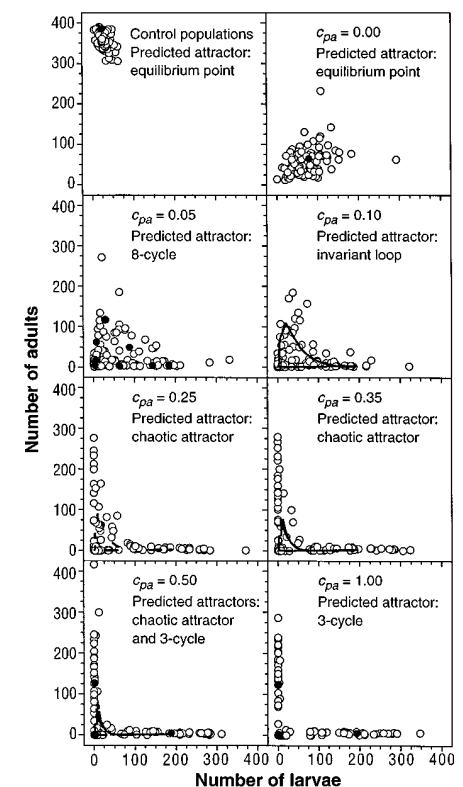

Fig. 3. Phase-space graphs of the data for t = 10 to 40 (open circles) together with the deterministic model attractors (solid circles, points, or loops) shown projected onto the adult-larval plane.

exponent is 0, which is consistent with a quasiperiodic attractor that forms an invariant loop in phase space. In the $c_{pa} = 0.25$ and $c_{pa} = 0.35$ treatments, the Liapunov exponent is positive and the attractors are chaotic. A region of multiple attractors (chaos and 3-cycles) is associated with the $c_{pa} = 0.50$ treatment. The stochastic variability of larvae and adults in the c_{pa}-manipulated treatments was larger than that of the unmanipulated control treatment as measured by the estimated noise variances (main diagonal in the Σ matrices) (15).

Despite the effects of stochasticity, which are always present in experimental populations, a close examination of the data reveals features of the predicted deterministic attractors. The time-series data for one replicate culture of each experimental treatment are given in Fig. 2. Comparison with the control shows that the experimental manipulations had a destabilizing effect on the population dynamics. For the control cultures, the model forecasts an asymptotic approach to a stable equilibrium with slowly increasing adult numbers. For $c_{pa} = 0.0$, the model predicts an oscillatory approach to equilibrium, with approximately equal numbers of insects in all three life stages. For $c_{pa} = 1.0$, a distinctive 3-cycle is predicted, with a repeating high-low-low pattern. These predictions are supported by the data.

The complex deterministic attractors forecast for the remaining treatments are more clearly visualized in phase space. In this case, phase space is three-dimensional with state variables L_t, P_t, and A_t. However, because P_t is a constant multiple of L_{t-1}, the features of the attractors are adequately seen when projected onto the L_t-A_t plane.

Data points for all replicates of each treatment are plotted in the projected phase planes in Fig. 3. To deemphasize the presence of transients (and hence better discern the features of the asymptotic attractors), we omitted the first 10 data points in these plots. The control and $c_{pa} = 0.0$ treatments show tight clusters of data points, as is consistent with the model prediction of a stable equilibrium (with noise). The $c_{pa} = 0.0$ cluster is less tightly packed in phase space than is the control, reflecting the increased stochastic variability of the c_{pa}-manipulated cultures. The $c_{pa} = 0.05$ and $c_{pa} = 0.10$ treatments show different patterns of data points, which are consistent with the predicted invariant loops. In the $c_{pa} = 0.10$ plot, the invariant loop is displayed with the data; in the $c_{pa} = 0.05$ plot, the model forecasts period locking on the invariant loop with period 8, as shown. For $c_{pa} = 0.25$, the data are scattered around the predicted chaotic attractor, which consists

of several islands of points. In the $c_{pa} = 0.35$ plot, the data are distributed in the L-A plane in a manner similar to the predicted chaotic attractor. For the treatments $c_{pa} = 0.50$ and $c_{pa} = 1.0$, the data are distributed tightly along the L and A axes, as predicted by the chaotic attractor and 3-cycles shown. A close examination of these plots reveals a clustering of the data around the displayed cycle points.

The experimental confirmation of nonlinear phenomena in the dynamics of the laboratory beetle lends credence to the hypothesis that fluctuations in natural populations might often be complex, low-dimensional dynamics produced by nonlinear feedbacks. In our study, complex dynamics were obtained by "harvesting" beetles to manipulate rates of adult mortality and recruitment. For applied ecology, the experiment suggests adopting a cautious approach to the management or control of natural populations, based on sound scientific understanding. In a poorly understood dynamical population system, human intervention—such as changing a death rate or a recruitment rate—could lead to unexpected and undesired results.

REFERENCES AND NOTES

1. M. P. Hassell and R. M. May, Eds., *Population Regulation and Dynamics* (Cambridge Univ. Press, Cambridge, 1990).
2. R. Pool, *Science* **243**, 310 (1989).
3. H. Tong and R. L. Smith, *J. R. Statist. Soc. B* **54**, 301 (1992).
4. H. C. J. Godfray and B. T. Grenfell, *Trends Ecol. Evol.* **8**, 43 (1993).
5. A. Hastings, C. L. Hom, S. Ellner, P. Turchin, H. C. J. Godfray, *Annu. Rev. Ecol. Syst.* **24**, 1 (1993).
6. S. Ellner and P. Turchin, *Am. Nat.* **145**, 343 (1995).
7. P. Kareiva, in *Perspectives in Ecological Theory,* J. Roughgarden, R. M. May, S. A. Levin, Eds. (Princeton Univ. Press, Princeton, NJ, 1989).
8. H. C. J. Godfray and S. P. Blythe, *Philos. Trans. R. Soc. London Ser. B* **330**, 221 (1990).
9. R. M. May, *Science* **186**, 645 (1974).
10. _____ and G. F. Oster, *Am. Nat.* **110**, 573 (1976).
11. Biologists have long used flour beetles of the genus *Tribolium* as a research tool to explore the dynamics of populations. The combination of high rates of reproduction, short life cycle (4 to 6 weeks from egg to adult), ease of culture, and a life history that includes strong nonlinear life-stage interactions (cannibalism) make the beetle a good laboratory system [A. Sokoloff, *The Biology of* Tribolium (Oxford Univ. Press, Oxford, vol. 1–3, 1972, 1974, 1977); R. F. Costantino and R. A. Desharnais, *Population Dynamics and the* Tribolium *Model: Genetics and Demography* (Springer-Verlag, New York, 1991)].
12. B. Dennis, R. A. Desharnais, J. M. Cushing, R. F. Costantino, *Ecol. Monogr.* **65**, 261 (1995).
13. R. F. Costantino, J. M. Cushing, B. Dennis, R. A. Desharnais, *Nature* **375**, 227 (1995).
14. H. Tong, *Non-linear Time Series: A Dynamical System Approach* (Oxford Univ. Press, Oxford, 1990).
15. The maximum likelihood parameter estimates in the deterministic skeleton, estimated using all of the data, are $b = 6.598$, $c_{el} = 1.209 \times 10^{-2}$, $c_{ea} = 1.155 \times 10^{-2}$, and $\mu_l = 0.2055$. Using only the control cultures, we also obtained $c_{pa} = 4.700 \times 10^{-3}$ and $\mu_a = 7.629 \times 10^{-3}$, where μ_a was estimated directly from numbers of dead adults. The maximum likelihood estimates in the variance-covariance matrices are $\sigma_{11} = 0.3412$, $\sigma_{22} = 0.2488$, $\sigma_{33} = 1.627 \times 10^{-4}$, $\sigma_{12} = 7.312 \times 10^{-2}$, $\sigma_{13} = -1.719 \times 10^{-3}$, and $\sigma_{23} = 3.374 \times 10^{-4}$ for Σ-control, and $\sigma_{11} = 0.7731$, $\sigma_{22} = 0.1085$, $\sigma_{33} = 0.1031$, $\sigma_{12} = -1.262 \times 10^{-2}$, $\sigma_{13} = -4.638 \times 10^{-2}$, and $\sigma_{23} = 5.113 \times 10^{-3}$ for Σ-manipulated.
16. A. A. Berryman and J. A. Millstein, *Trends Ecol. Evol.* **4**, 26 (1989).
17. Supported in part by NSF grants DMS-9306271, DMS-9319073, DMS-9625576, and DMS-9616205.

14 August 1996; accepted 22 October 1996

A Mouse Model with Features of Familial Combined Hyperlipidemia

Lori Masucci-Magoulas, Ira J. Goldberg, Charles L. Bisgaier, Humaira Serajuddin, Omar L. Francone, Jan L. Breslow, Alan R. Tall*

Familial combined hyperlipidemia (FCHL) is a common inherited lipid disorder, affecting 1 to 2 percent of the population in Westernized societies. Individuals with FCHL have large quantities of very low density lipoprotein (VLDL) and low density lipoprotein (LDL) and develop premature coronary heart disease. A mouse model displaying some of the features of FCHL was created by crossing mice carrying the human apolipoprotein C-III (*APOC3*) transgene with mice deficient in the LDL receptor. A synergistic interaction between the apolipoprotein C-III and the LDL receptor defects produced large quantities of VLDL and LDL and enhanced the development of atherosclerosis. This mouse model may provide clues to the origin of human FCHL.

Familial combined hyperlipidemia is the most common genetic dyslipidemia and is characterized by large amounts of VLDL or LDL or both, as well as apolipoprotein B

(APOB), and small amounts of high density lipoprotein (HDL) (1, 2). FCHL affects about 5% of all individuals with coronary heart disease and 10% of individuals with